# On the choice of optimal conformation in linear free-energy relationships. Reactivity of 2-[(carboxymethyl)sulfanyl]-4-oxo-4-arylbutanoic acids with diphenyldiazomethane

Branko J. Drakulić [a,*], Aleksandar D. Marinković [b], Ivan O. Juranić [a]

[a] *Department of Chemistry, Institute of Chemistry, Technology and Metallurgy, University of Belgrade, Njegoševa 12, 11000 Belgrade, Serbia*
[b] *Faculty of Technology and Metallurgy, University of Belgrade, Karnegijeva 4, 11000 Belgrade, Serbia*

A B S T R A C T

Rate constants for the esterification of eleven 2-[(carboxymethyl)sulfanyl]-4-oxo-4-arylbutanoic acids with diphenyldiazomethane in ethanol at 30 °C were determined, and correlated with substituent constants using classical Hammett and related methods. Statistically valid results for the *para*-substituted compounds were obtained by the Swain–Lupton approach. The compounds studied had significant conformational mobility due to seven rotatable bonds in their backbone. Going beyond the classical Hammett approach, we established a relatively fast procedure to find the optimal conformations that can be used in linear free-energy relationships, combining molecular dynamics with semiempirical calculations, and calculations using a higher level of theory (DFT and MP2). Fair correlations were observed with frontier orbitals, allowing inclusion of *ortho*-substituted derivatives and clarifying artifact-like data, as perceived by the Hammett-type approach.

© 2011 Elsevier Ltd. All rights reserved.

2-[(Carboxymethyl)sulfanyl]-4-oxo-4-arylbutanoic acids exert antiproliferative activity and significant selectivity (tumor vs healthy human cells).[1] The title compounds are a unique chemotype so far, although reasonably similar compounds have been reported as immunosuppressors,[2] and recently as allosteric ligands for 3-phosphoinositide-dependent protein kinase 1 (PDK1).[3] Within an ongoing study on the structure–activity relationships of the title compounds, we examined the transmission of substituent effects through the molecular skeleton, and the reactivity of the carboxyl groups. With this rationale, the rate constants of esterification of eleven compounds **1–11** (Table 1) with diphenyldiazomethane (DDM) were determined using the spectrophotometric method introduced by Roberts et al.[4,5] DDM reacts with carboxylic acids as shown in Scheme 1a. In an alcohol as solvent, a competing reaction (etherification of the alcohol) occurs[6] as shown in Scheme 1b.

The compounds chosen for this study had a simple substitution pattern, comprising alkyl and halogen substituents, mainly in *para* positions.[7] Still, a straightforward relationship between the rate constants and a substituent effect was not observed. Probably this can be attributed to two factors. The first is lack of conjugation between the aryl moiety and the carboxyl groups that underwent esterification, and the second is the flexibility of the molecules

studied. Transmission of electronic effects through $-S-CH_2-$[8] and $-CH_2-CH_2-$[9] moieties has been documented. Rate constants for esterification of dicarboxylic acids with DDM have been reported.[10]

Using classical Hammett and related approaches, a statistically fair correlation was derived using the Swain–Lupton method,[11,12] excluding the *ortho*-substituted derivative **11**, see (Eq. 1), Table S1, and Figure S1 in the Supplementary data.

$$\log k_2 = 0.0395 \ (\pm0.0166) \ F - 0.3031 \ (\pm0.0265) \ R$$
$$- 0.5592 \ (\pm0.0066) \tag{1}$$

$r = 0.9807$, sd = 0.0098, $n = 10$, $F = 88.50$, $F_{significance} = 1.1 \times 10^{-5}$; compound **11** is anomalous.
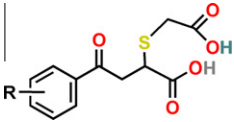
The resonance effect appears to be one order of magnitude higher than the field effect. For the 3,4-di-Me-substituted derivative **10**, doubled values for both $F$ and $R$ were used, because the Swain–Lupton substituent constants are position independent. For compounds **3**, **4**, **5**, and **9**, $R^+$ values were used; this can be explained by hyperconjugation for alkyl-substituted compounds. The $R^-$ fits compound **6** best to (Eq. 1), an inconsistency that will be discussed below.

The title compounds are significantly flexible in standard solvents. To illustrate this, the range of surface area[14] of molecules obtained from 15 nanosecond molecular dynamics (MD) trajectories in an implicit solvent is given in Table S1 in the Supplementary data. The majority of the conformations obtained had energies higher than 5 kcal/mol compared to the global minimum, as perceived by

---

* Corresponding author. Tel.: +381 11 3336738; fax: +381 11 2636061.
 *E-mail address:* bdrakuli@chem.bg.ac.rs (B.J. Drakulić).

**Table 1**
Logarithmic values of second-order rate constants for esterification of **1–11** with DDM; polar surface area of molecules in chosen conformation (PSA); values of highest occupied molecular orbitals (HOMO) obtained at the semiempirical PM6 level; and HOMO–LUMO differences obtained by DFT and MP2 calculations



| Compound | R- | $\log k_2$ | $\log(k/k_0)$ | PSA (Å$^2$) | PM6 HOMO (eV) | DFT HOMO–LUMO diff (eV) | MP2 HOMO–LUMO diff (eV) |
|---|---|---|---|---|---|---|---|
| **1** | H- | −0.5498 | − | 220.8 | −9.660 | −4.6458 | −11.4538 |
| **2** | 4-Me- | −0.5017 | 0.9125 | 215.6 | −9.662 | −4.5438 | −11.1254 |
| **3** | 4-Et- | −0.4698 | 0.8545 | 222.9 | −9.694 | −4.6575 | −11.1863 |
| **4** | 4-*i*-Pr- | −0.4609 | 0.8383 | 227.4 | −9.731 | −4.9868 | −11.3050 |
| **5** | 4-*n*-Bu- | −0.4908 | 0.8927 | 224.6 | −9.692 | −4.8537 | −11.2236 |
| **6** | 4-*t*-Bu- | −0.5560 | 1.0112 | 192.0 | −9.445 | −4.1190 | −10.8930 |
| **7** | 4-F- | −0.4225 | 0.7685 | 221.7 | −9.898 | −5.0610 | −11.7102 |
| **8** | 4-Cl- | −0.4828 | 0.8781 | 204.1 | −9.605 | −4.5242 | −11.4141 |
| **9** | 4-Br- | −0.4547 | 0.8270 | 213.6 | −9.776 | −4.7500 | −11.3616 |
| **10** | 3,4-Di-Me- | −0.4342 | 0.7897 | 237.7 | −9.583 | −4.9122 | −11.2554 |
| **11** | 2,5-Di-Me- | −0.4145 | 0.7540 | 228.4 | −9.428 | −5.1182 | −11.8775 |
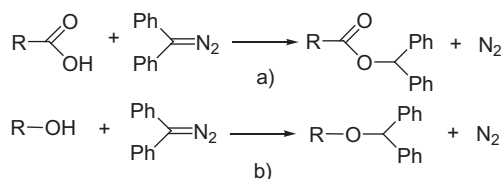


**Scheme 1.** (a) General reaction for the esterification of carboxylic acids with diphenyldiazomethane (DDM). (b) General reaction for the etherification of alcohols with diphenyldiazomethane (DDM).

the ABF procedure used, see Figure S2 in the Supplementary data. All the compounds exerted similar conformational mobility. This is illustrated by the ratio of the range of 3D dependent surface areas to the molecular weights of the compounds (Table S1 in the Supplementary data), and is expected for the molecules having the same core structure and a similar number of rotatable bonds. Some successful attempts to account for the conformational mobility of molecules in linear free-energy relationships (LFER) can be found in the literature.[15] Such studies describe molecules having not more than two rotatable bonds; substituent effects were accounted for by using classical Hammett substituent constants and the Yukawa–Tsuno equation. The conformational adaptation of substituents was also described.[16]

As no other literature reports exist on transmission of substituent effects for flexible, partially conjugated molecules, we tried to find a way to establish a correlation on rational grounds. We aimed first to find the conformations that could be used for the correlations, and then to obtain descriptors that are specific for particular conformations, and that describe the entire molecule. Frontier orbitals, often used to quantify the electrophilicity or nucleophilicity of entire molecules in their reactions, appeared to be a logical choice. Classical geometry optimization using fast semiempirical methods, or significantly slower and computationally more demanding methods on a higher level of theory (DFT, ab initio) when applied to compounds having significant conformational mobility have obvious drawbacks. The main obstacle is the heavy dependence of the output conformation on the choice of the starting one. Local minima can be readily obtained in this way, and for semiempirical methods the difference of energies among the minima obtained is within the confidence limit of the method.

Methods using a higher level of theory are free of the drawback of the uncertainty in the energy differences among local minima, but are very time-demanding. Inspired by our on-going study of the free-energy landscapes of the title compounds in various explicit solvents, aimed to derive biologically relevant conclusions,[17] we employed a similar procedure,[18] using implicit solvation, to find the global energy minima, and to speed-up the computation. Each molecule was submitted to a 15 ns MD simulation in implicit ethanol at 300 K. To enhance sampling and to map the free energy surface, an adaptive biasing force (ABF)[26] calculation was used. Two collective variables that map the conformational space of molecules in the most comprehensive way, were chosen on the basis of previous calculations (data not shown): the distance between centroids defined on aroyl phenyl and distal carboxyl groups; and the radius of gyration of all heavy atoms, including substituents (Figure S3 in the Supplementary data). Energy minima were extracted from free-energy surfaces. The conformation closest to the free-energy minimum was found from the collective variables trajectory file. To remove artifacts stemming from molecular mechanics (small deviations of planarity in phenyl rings, bond lengths), and to retain the conformations most similar to those obtained by molecular dynamics, all structures were optimized at the semiempirical PM6 level[27] to acceptable root-mean-square gradients in the implicit solvent,[28] and in a vacuum. Comparing the initial conformations obtained as MD minima and the corresponding optimized ones, the largest root-mean-square deviation (RMSD) of the backbone atoms (excluding substituents) was 0.92 (Table S1 in Supplementary data). The main contribution to RMSD, for all molecules, arose from the position of atoms in the phenyl rings, that is, Ph to C(O) torsion (Figure S4 in the Supplementary data). The highest occupied molecular orbitals (HOMOs) derived from the semiempirical calculations correlated well with experimentally obtained rate constants for the *para*-substituted congeners **2–9** ((Eq. 2) and Figure S5 in the Supplementary data).

$$\log(k/k_0) = 0.5197\ (\pm 0.0660)\ \text{HOMO}_{(PM6)}$$
$$+\ 5.9080\ (\pm 0.6392) \tag{2}$$

$r = 0.9549$, sd = 0.023, $n = 8$, $F = 62.066$, $F_{significance} = 2 \times 10^{-4}$; outliers **10** and **11**.

Compounds having *meta–para* (**10**) and *ortho–meta* (**11**) substitution patterns are obviously anomalous. Single point calculations,

on structures derived by semiempirical calculations were performed using DFT and MP2 methods, both in an implicit solvent[29] and in vacuum. Fair correlations were obtained using HOMO–LUMO energy differences derived with DFT ((Eq. 3) and Figure S6 in the Supplementary data), and MP2 ((Eq. 4) and Figure S7 in the Supplementary data) methods, giving best statistical results for the DFT method.

$$\log (k/k_0) = 0.2305\ (\pm 0.0364)\ \text{HOMO–LUMO\_diff}_{(DFT)}$$
$$+ 1.9480\ (\pm 0.1735) \tag{3}$$

$r = 0.9128$, sd = 0.033, $n = 10$, $F = 39.991$, $F_{\text{significance}} = 2 \times 10^{-4}$.

$$\log (k/k_0) = 0.2991\ (\pm 0.0503)\ \text{HOMO–LUMO\_diff}_{(MP2)}$$
$$+ 3.4501\ (\pm 0.5708) \tag{4}$$

$r = 0.8494$, sd = 0.043, $n = 10$, $F = 20.720$, $F_{\text{significance}} = 0.001$.

The exclusion of compound **10** yielded somewhat better statistics ($r = 0.9218$, $F = 39.569$). For semiempirical calculations, in the absence of implicit solvation, no correlation was found. Similarly, correlations having significantly lower statistical quality were obtained by DFT and MP2 calculations, using data for which implicit solvation was not applied (data not shown).

It should be noted that the initially observed rate constant for derivative **6** looks erroneous, because only the Swain–Lupton R⁻ fits this compound to a statistically valid correlation. The experiments were repeated, giving very reproducible results. Even at the semiempirical level of calculation it became clear that this derivative fits well to the correlation, the same was observed for DFT and MP2 calculations (see Table S2 in the Supplementary data). Also, a trend in the relationship between the 3D dependent polar surface area of the compounds, in their respective conformations, and rate constants was evident (Table S1 and Figure S8 in the Supplementary data). Such a trend cannot be observed for the average PSA of the compounds. So far we cannot offer a rationale for this observation. The random choice of conformations from the comparable regions of the free-energy landscape, different from the minimum, does not show any statistically valid correlations, or a trend that can be observed visually (data not shown).

Ionization constants of **1–11** were estimated[30] (Table S4 in the Supplementary data), and a pH profile typical for these compounds is exemplified in Figure S9 in the Supplementary data. We have observed a trend in the correlation between the estimated p$K_a$ values and the experimentally obtained rate constants for esterification with DDM (Figure S10 in the Supplementary data). Rate constants for esterification were determined in dry ethanol, while p$K_a$ estimates were obtained using conditions resembling physiological ones, so we found a fair agreement. At this point it should be noted that, apart from the modeling that comprises the main part of this text, the correspondence between the two data sets of results shows again the validity of the Hammett approach. This topic has been nicely evaluated by Jaffe[31,32] and the many articles that followed his study.

Having in hand the results described, the first questions that arose and which looked attractive were whether the product of the reactions could be modeled in the same way; and whether some correlation could be obtained from such calculations; using the products of esterification alone, or by comparing conformation-dependent whole-molecular descriptors for both the initial acids and products. Relying on real 'in flask' data, the products cannot be modeled in a simple way. The rate constants were determined under pseudo-first order conditions, using a large excess of the acids, and we have no indication whether one or both carboxyl groups are esterified. It has been shown that during esterification of acids with DDM in alcohols, about 60% of the DDM is involved with esterification of the carboxyl groups, while the rest reacts with the alcohol.[6]

In conclusion, we have found that conformation-specific descriptors of flexible molecules are suitable for linear free-energy relationships, and suggest a novel procedure for finding the appropriate conformation. Frontier orbitals appear as suitable descriptors for linear free-energy relationships of esterification of the title compounds with DDM, allowing the inclusion of an *ortho*-substituted derivative. The method was tested on a small set of molecules; further study in this direction is in progress. To the best of our knowledge, a similar approach to LFER has not been described in the literature.

## Acknowledgments

## Supplementary data

Supplementary data associated with this article can be found, in the online version, at doi:10.1016/j.tetlet.2011.11.097.

## References and notes

1. Drakulić, B. J.; Juranić, Z. D.; Stanojković, T. P.; Juranić, I. O. *J. Med. Chem.* **2005**, *48*, 5600–5603.
2. Kawashima, Y.; Kameo, K.; Kato, M.; Hasegawa, M.; Tomisawa, K.; Hatayama, K.; Hirono, S.; Moriguchi, I. *Chem. Pharm. Bull.* **1992**, *40*, 774–777.
3. Hindie, V.; Stroba, A.; Zhang, H.; Lopez-Garcia, L. A.; Idrissova, L.; Zeuzem, S.; Hirschberg, D.; Schaeffer, F.; Jørgensen, T. J. D.; Engel, M.; Alzari, P. M.; Biondi, R. M. *Nat. Chem. Biol.* **2009**, *5*, 758–764.
4. Roberts, J. D.; McElhill, E. A.; Armstrong, R. *J. Am. Chem. Soc.* **1949**, *71*, 2923–2926.
5. *Experimental procedures*: Compounds **1–11** (Table 1) were synthesized and characterized as reported previously,[1] showing >98% purity. Rate constants for the reactions of compounds **1–11** with DDM were determined by spectroscopic methods, in ethanol, using a Shimadzu UV-1700 spectrophotometer. The absorbance was measured at 525 nm, and 30 ± 0.05 °C, in 1 cm cells. The second-order rate constants were obtained by dividing the pseudo-first-order rate constants by the concentration of compound tested (**1–11** at a concentration of 0.06 mol/dm³, DDM at a concentration of 0.006 mol/dm³). Three to five rate determinations were performed. The second-order rate constants agreed within 3% of the mean values.
6. Roberts, J. D.; Watanabe, W.; McMahon, R. E. *J. Am. Chem. Soc.* **1951**, *73*, 760–765.
7. Choosing substituents for this study, we were guided by both biological and physico-chemical rationales. Regarding biological activity, alkyl substituted compounds are significantly more potent than halogen substituted, and *ortho*-alkyl substituted compounds exert both better potency and selectivity than the others. From the physico-chemical point of view, and on the basis of literature, linearity in LFER is always more challenging to obtain for compounds substituted by similar substituents (i.e., a set of alkyl substituted compounds), than for sets having substituents with a wide variety of electron-donating or electron-withdrawing properties.
8. (a) Pasto, D. J.; McMillan, D.; Murphy, T. *J. Org. Chem.* **1965**, *30*, 2688–2691; (b) Pettit, L. D.; Royston, A.; Sherrington, C.; Whewell, R. J. *J. Chem. Soc. B* **1968**, 588–590.
9. (a) O'Ferrall, R. M.; Miller, S. I. *J. Am. Chem. Soc.* **1963**, *85*, 2440–2444; (b) Fuchs, R.; Kaplan, C. A.; Bloomfield, J. J.; Hatch, L. F. *J. Org. Chem.* **1962**, *27*, 733–736.
10. (a) Smith, H. A.; Hunt, P. P. *J. Am. Chem. Soc.* **1958**, *81*, 590–592; (b) Mišić-Vuković, M.; Radojković-Veličković, M.; Jezdić, V. *J. Chem. Soc., Perkin Trans. 2* **1990**, 109–112.
11. Swain, C. G.; Lupton, E. C. *J. Am. Chem. Soc.* **1968**, *90*, 4328–4337.
12. Swain–Lupton substituent constants, modified by Hansch et al.,[13] were used.
13. Hansch, C.; Leo, A.; Hoekman, D. *Exploring QSAR, in Hydrophobic, Electronic and Steric Constants*; American Chemical Society: Washington DC, 1995.
14. Vistoli, G.; Pedretti, A.; Villa, L.; Testa, B. *J. Med. Chem.* **2005**, *48*, 4947–4952.
15. See for example: Fujio, M.; Kim, H.-J.; Uddin, Md. K.; Yoh, S.-D.; Rappoport, Z.; Tsuno, Y. *J. Phys. Org. Chem.* **2002**, *15*, 330–342.
16. Inagaki, S.; Okajima, T.; Yamamura, K.; Miyake, H.; Nakasuji, K.; Murata, I. *Bull. Chem. Soc. Jpn.* **1990**, *63*, 2099–2100.

17. Drakulić, B. J.; Pedretti, A.; Zloh, M.; Slavnić, V.; Juranić, I. O.; Dabović, M. M. *Range and Sensitivities of 2-[(Carboxymethyl)sulfanyl]-4-oxo-4-arylbutanoic Acids Property Spaces. Part 2. Multidimensional Free Energy Landscapes*, 18th European Symposium on Quantitative Structure–Activity Relationships, Discovery Informatics & Drug Design, Sep 19–24, 2010; Final Program & Abstract Book, pp 278–279.

18. Initial conformations of **1–11** were generated from SMILES notation by OMEGA.[19] The MMFF94s[20] force field was used. The arbitrary, *S*-configuration on the stereogenic carbon was assigned for all compounds. All structures are optimized by the semiempirical molecular orbital PM6 method, as applied in MOPAC2009,[21] in implicit solvent (COSMO) to the root mean square gradient below 0.001 kcal/mol/Å. For all calculations ethanol was used as the implicit solvent. PDB and PSF files were generated using Gasteiger charges and the CHARMM force field. Implicit solvation in NAMD 2.8[22] by the Generalized Born model of Onufriev, Bashford and Case (GB-OBC) was used. Systems were heated from 0 to 300 K in 10,000 steps. Fifteen nanoseconds molecular dynamics with constant temperature 300 (±20) K, integration of Newton's equation each 1 fs according to Verlet's algorithm, and electrostatic interactions recalculated each 4 iterations were performed. Periodic boundary conditions were not applied. Simulation space partitioning was applied using something bigger cut-offs comparing to similar simulations in explicit solvent, as suggested for GB-OBC; cut-off 18.000, switch distance 16.00, pair list distance 19.000 Å. The trajectory frequency was set to 10,000, obtaining 14,990 frames during simulation. Adaptive-biasing force calculations were applied during productive runs. Collective variables were collected after 500 samples, with a frequency of 1. Boundaries were determined from previous runs in explicit solvents. The Abf-integrate was used for generating potential mean force files from NAMD ABF records. An in-house script was used for extraction of free-energy minima in each file. Free-energy surfaces were visualized by GNUplot 4.4.2. Colvars trajectory files were truncated using the Python script[23] to obtain a number of lines equal to the number of frames collected during simulation. From those files distance versus radius of gyration (rgyr) plots were made. Conformations having minimal Euclidian distance to coordinates of energy minimum were used for further calculations. Extracted conformations were optimized using a semiempirical molecular orbital PM6 method, in Cartesian coordinates to the root mean square gradient below 0.1 kcal/mol/Å in vacuum, or in implicit solvent (COSMO). Eigenvector following optimizer was used. Single point calculations were performed on resulting conformations using DFT (B3LYP), and MP2 methods, with the 6–311G** basis set, in vacuum or in implicit solvent (PCM, 300 K). Cut-offs on forces and step size to determine convergence were tightened using the 'Tight' option. All values of frontier orbitals given in Tables 1 and S1–S3 are in electron-volts. DFT and MP2 calculations were performed with Gaussian03.[24] Superimposition of

molecules, as well as calculated 3D-dependent solvent assessable, and polar surface areas of molecules, were obtained with a VegaZZ 2.4.0.[25] A probe of 1.4 Å radius, and dot density of 100 was used. All molecular dynamics simulations were run on a multi-node Linux based cluster equipped with 2 × quad core Intel Xeon-E5345 @ 2.33 GHz processors, with NAMD 2.8 compiled under Charmrun.

19. (a) Boström, J. *J. Comput. Aided Mol. Des.* **2001**, *15*, 1137–1152; (b) Boström, J.; Greenwood, J. R.; Gottfries, J. *J. Mol. Graphics Modell.* **2003**, *21*, 449–462 (www.eyesopen.com).

20. Halgren, T. A. *J. Comput. Chem.* **1999**, 720–729.

21. Stewart, J. J. P. *J. Comput. Aided Mol. Des.* **1990**, *4*, 1–105. MOPAC2009, Stewart, J. J. P.; Stewart Computational Chemistry, Colorado Springs, CO, USA, 2009, http://OpenMOPAC.net.

22. cattraj.py script by Bjoern Erik Sven Olausson, http://olausson.de.

23. Frisch, M. J.; Trucks, G. W.; Schlegel, H. B.; Scuseria, G. E.; Robb, M. A.; Cheeseman, J. R.; Montgomery, J. A.; Vreven, T., Jr.; Kudin, K. N.; Burant, J. C.; Millam, J. M.; Iyengar, S. S.; Tomasi, J.; Barone, V.; Mennucci, B.; Cossi, M.; Scalmani, G.; Rega, N.; Petersson, G. A.; Nakatsuji, H.; Hada, M.; Ehara, M.; Toyota, K.; Fukuda, R.; Hasegawa, J.; Ishida, M.; Nakajima, T.; Honda, Y.; Kitao, O.; Nakai, H.; Klene, M.; Li, X.; Knox, J. E.; Hratchian, H. P.; Cross, J. B.; Adamo, C.; Jaramillo, J.; Gomperts, R.; Stratmann, R. E.; Yazyev, O.; Austin, A. J.; Cammi, R.; Pomelli, C.; Ochterski, J. W.; Ayala, P. Y.; Morokuma, K.; Voth, G. A.; Salvador, P.; Dannenberg, J. J.; Zakrzewski, V. G.; Dapprich, S.; Daniels, A. D.; Strain, M. C.; Farkas, O.; Malick, D. K.; Rabuck, A. D.; Raghavachari, K.; Foresman, J. B.; Ortiz, J. V.; Cui, Q.; Baboul, A. G.; Clifford, S.; Cioslowski, J.; Stefanov, B. B.; Liu, G.; Liashenko, A.; Piskorz, P.; Komaromi, I.; Martin, R. L.; Fox, D. J.; Keith, T.; Al-Laham, M. A.; Peng, C. Y.; Nanayakkara, A.; Challacombe, M.; Gill, P. M. W.; Johnson, B.; Chen, W.; Wong, M. W.; Gonzalez, C.; Pople, J. A. *GAUSSIAN 03, Revision C.02*; Gaussian, Inc.: Pittsburgh, PA, 2003.

24. Pedretti, A.; Villa, L.; Vistoli, G. *J. Comput. Aided Mol. Des.* **2004**, *18*, 167–173. http://www.ddl.unimi.it.

25. Phillips, J. C.; Braun, R.; Wang, W.; Gumbart, J.; Tajkhorshid, E.; Villa, E.; Chipot, C.; Skeel, R. D.; Kalé, L.; Schulten, K. *J. Compd. Chem.* **2005**, *26*, 1781–1802.

26. Henin, J.; Fiorin, G.; Chipot, C.; Klein, M. L. *J. Chem. Theory Comput.* **2010**, *6*, 35–47.

27. Stewart, J. J. P. *J. Mol. Mod.* **2007**, *13*, 1173–1213.

28. Klamt, A.; Schüümann, G. *J. Chem. Soc., Perkin Trans. 2* **1993**, 799–805.

29. Miertus, S.; Scrocco, E.; Tomasi, J. *Chem. Phys.* **1981**, *55*, 117–119.

30. ADMET Predictor, version 5.5.17; Simulations Plus, Inc.; 2011 (http://www.simulations-plus.com).

31. Jafee, H. H. *J. Chem. Phys.* **1953**, *21*, 415–419.

32. Jafee, H. H. *Chem. Rev.* **1953**, *53*, 191–261.